Polymer micelle-directed growth of BaCO$_3$ spiral nanobelts

Wenjie Zhu, Chunhua Cai, Jiaping Lin,* Liquan Wang, Lili Chen, Zeliang Zhuang

Shanghai Key Laboratory of Advanced Polymeric Materials, State Key Laboratory of Bioreactor Engineering, Key Laboratory for Ultrafine Materials of Ministry of Education, School of Materials Science and Engineering, East China University of Science and Technology, Shanghai 200237, China

* E-mail: jlin@ecust.edu.cn (J. Lin)

Electronic Supplementary Material (ESI) for Chemical Communications
This journal of (c) The Royal Society of Chemistry 2012

1. Experimental Section

Materials. *N*-isopropylacrylamide (NIPAM, 97%, Aldrich) was recrystallized from n-hexane prior to use. 2, 2'-Azobisisobutyronitrile (AIBN, CR) was recrystallized from ethanol and dried at room temperature under vacuum. 2-Aminoethanethiol hydrochloride (AET·HCl) was purchased from Aldrich and used without further purification. γ-benzyl-L-glutamate-N-carboxyanhydride (BLG–NCA) was synthesized by synthesized by phosgenation of of γ-benzyl L-glutamate according to the method proposed by Blout and Karlson.[1] Tetrahydrofuran (THF), hexane and 1,4-dioxane were refluxed with sodium and distilled immediately before use. $BaCl_2 \cdot 2H_2O$ and $(NH_4)_2CO_3$ and other reagents are of analytical grade and used without further purification. Deionized water (DIW) was made in a Millipore Super-Q Plus Water System to a level of 18 MΩ resistance. All glassware for crystallization experiment (glass bottles and small pieces of glass substrates) was cleaned and sonicated in ethanol for 5 min. It was then rinsed with DIW, further soaked in a H_2O-HNO_3(65%)-H_2O_2 (1:1:1, V/V/V) solution, and then rinsed with DIW. Afterward, it was dried in air with acetone. Dialysis bag (Membra-cel,3500 molecular weight cutoff) was provided by Serva Electrophoresis GmbH.

Synthesis of block copolymers. Monoamino-terminated PNIPAM (PNIPAM-NH_2) was synthesized by the free radical polymerization of NIPAM in methanol at 60 °C using AIBN as the initiator and AET·HCl as the chain transfer reagent.[2, 3] The number of repeat units and polydispersity indices (PDI) of PNIPAM was 45 and 1.57 respectively tested by GPC using THF as eluent and calibrated with polystyrene standards. PNIPAM-*b*-PBLG copolymers were synthesized by ring-opening polymerization of γ-benzyl-L-glutamate-N-carboxyanhydride (BLG-NCA) initiated by

Electronic Supplementary Material (ESI) for Chemical Communications
This journal of (c) The Royal Society of Chemistry 2012

the PNIPAM-NH$_2$. The composition of the PNIPAM-b-PBLG copolymer was determined by ^{1}H NMR spectra. The polydispersity indexes (PDI) of PNIPAM-b-PBLG were determined by gel permeation chromatography (GPC) in dimethylformamide (DMF). The results show that the repeat unit number of PBLG block is 229 and the PDI of PNIPAM-b-PBLG is 1.21. PNIPAM-b-PLGA block copolymers were prepared by hydrolyzation of PNIPAM-b-PBLG with potassium hydroxide (KOH).[4, 5] The complete deprotection of the benzyl group was confirmed by the disappearance of methylene proton peak (5.1 ppm) of PBLG block.

Preparation of polymer micelles. The copolymer solution was prepared by dissolving PNIPAM-b-PLGA copolymers with BaCl$_2$ in DIW. Raising the solution temperature leaded to the self-assembly of copolymers. In a typical procedure, 20 mg PNIPAM-b-PLGA was dissolved in 10 mL DIW firstly by the aid of sonication and NaOH. The pH value of the solution was carefully adjusted to about 8.0 by NaOH, HCl and DIW. The final solution volume was fixed at 20 mL. Then 24.4 mg (0.10 mmol) BaCl$_2$·2H$_2$O was added as the barium source of BaCO$_3$. After then the solution was filtered by using a 0.22 μm Millipore filter to remove impurities. To prepare the micelle, the solution was put in a 50 ^{o}C constant temperature oven for 24 hours. The morphology of copolymer micelles were characterized by using SEM. The average hydrodynamic size of the formed micelles is characterized by dynamic laser light scattering (DLS).

Mineralization. The mineralization was performed by a gas-diffusion method as described by Addadi et al.[6] Firstly, 5 mL of the polymer solution and some glass wafers were put in a 10 mL bottle. The bottle was covered by pierced parafilm and placed at a 5 L desiccator in a constant temperature

3

oven. After then, 6 g $(NH_4)_2CO_3$ in a bottle was placed at the bottom of the desiccator. For a certain time (typically 72 hours at 25^oC, 24 hours at $50\ ^oC$), the glass wafers were taken out, rinsed with DIW, and dried in air for further characterization.

Characterization. The crystals on the glass wafers were observed by scanning electron microscopy (SEM) (HITACHI-4800) operated at an accelerating voltage of 10 kV. Before the observation, the samples were sputtered by gold. The high-resolution transmission electron microscopy (HR-TEM) image and selective area electronic diffraction (SAED) were performed on a JEM-2100F operated at an accelerating voltage of 200 kV. The sample was prepared by transferring the crystals to a copper grid with carbon film and dried in air before the observation. The optical microscope micrographs were taken with an Olympus BH-2 optical microscope with a first-order red (gypsum) λ-plate. XRD patterns were recorded on Rigaku D/Max-2550V with Cu Kα radiation. Simultaneous thermogravimetry (TG) and differential scanning calorimetry (DSC) analysis were performed with a thermogravimetric analyzer (NETZSCH STA 409 PC/PG) at a heating rate of 10 ^oC/min from room temperature to 800 °C under nitrogen flow. Dynamic light scattering (DLS) measurement was performed using a commercial LLS spectrometer (ALV/CGS-5022) equipped with an ALV-High QE APD detector and an ALV-5000 digital correlator using a He-Ne laser (the wavelength λ=633 nm) as light source.

Electronic Supplementary Material (ESI) for Chemical Communications
This journal of (c) The Royal Society of Chemistry 2012

2. Supplementary Results

2.1 The micellization behavior of the PNIPAM-*b*-PLGA copolymers.

The PNIPAM-*b*-PLGA copolymers have a PNIPAM block and a PLGA block (marked in blue and red respectively, Figure S1a). Both of the blocks are soluble at room temperature. The PNIPAM block becomes insoluble above the lower critical solution temperature (about 32°C), causing the PNIPAM-*b*-PLGA copolymers self-assemble into micelles (Figure S1b). The SEM image displays the spherical micelles with diameters in the range 100 to 200 nm (Figure S1c). The DLS measurement shows a unimodal distribution with the R_h value of 99.2 nm, implying that the micelles are well-defined with a relatively uniform particle size (Figure S1d).
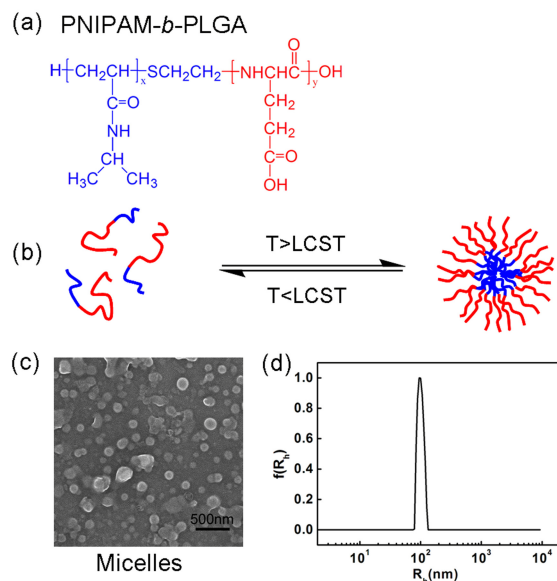

Figure S1. (a) the molecular formula of the PNIPAM-*b*-PLGA, (b) the scheme displaying the unimers-micelle transition in response to temperature variations, (c) a typical SEM image of PNIPAM-*b*-PLGA micelles obtained at 50 °C at a concentration of 1.0 g/L, (d) the corresponding hydrodynamic radius distribution $f(R_h)$ of the micelles determined at 90° scattering angle.

Electronic Supplementary Material (ESI) for Chemical Communications
This journal of (c) The Royal Society of Chemistry 2012

2.2 XRD analysis of the sample

The polymorph of the sample was examined by XRD, which indicates that the sample is the witherite phase in the orthorhombic phase and the Pmcn space group (JCPDS 45-1471).
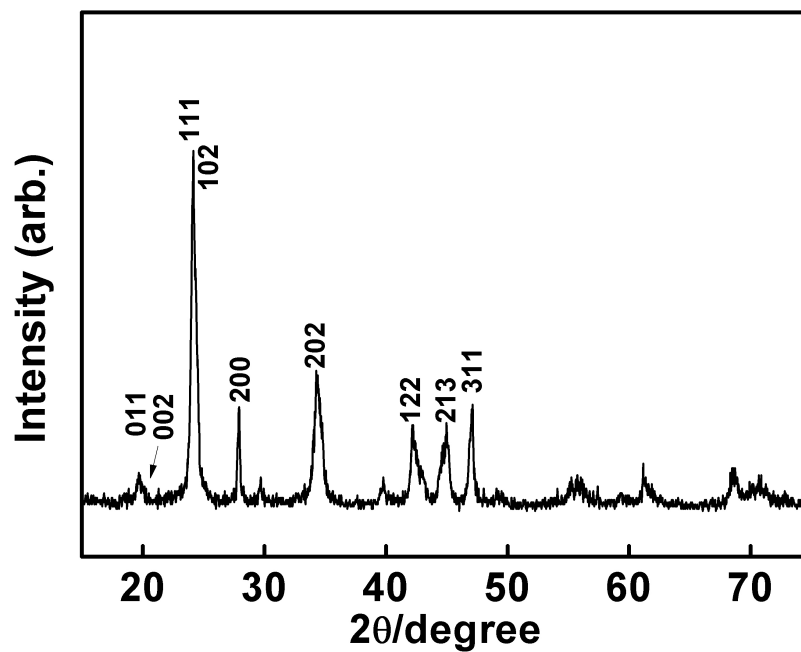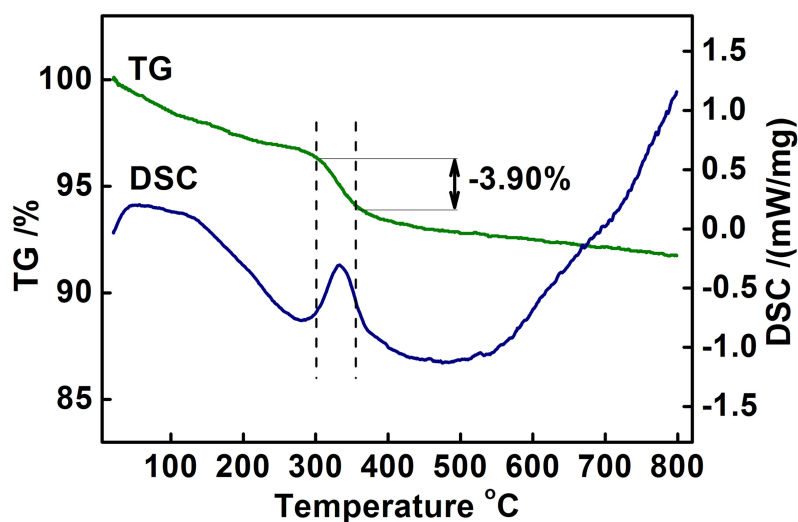

Figure S2. XRD pattern of $BaCO_3$ crystals obtained in the presence of PNIPAM-*b*-PLGA micelles at a concentration of 1.0 g/L at 50 $^{\circ}$C, and the Ba^{2+} concentration is 5 mM.

Electronic Supplementary Material (ESI) for Chemical Communications
This journal of (c) The Royal Society of Chemistry 2012

2.3 Thermal analysis of the witherite sample

Thermal analysis was applied to measure the content of the polymers in the witherite sample. TG curve shows a sharp weight-loss step at around 300 °C, which corresponds to the decomposition of the PNIPAM-*b*-PLGA copolymers. The decomposition is further certified by the corresponding endothermal peak in the DSC curve.


Figure S3. DSC/TG curves of the witherite crystals obtained in the presence of PNIPAM-*b*-PLGA micelles at a concentration of 1.0 g/L at 50 °C, and the Ba^{2+} concentration is 5 mM.

Electronic Supplementary Material (ESI) for Chemical Communications
This journal of (c) The Royal Society of Chemistry 2012

2.4 $BaCO_3$ crystallization under control of polymer unimers

At temperatures below the LCST, the PNIPAM block is soluble in aqueous solution. In this case, the formed $BaCO_3$ crystals are dendritic with diameters of tens micrometers.
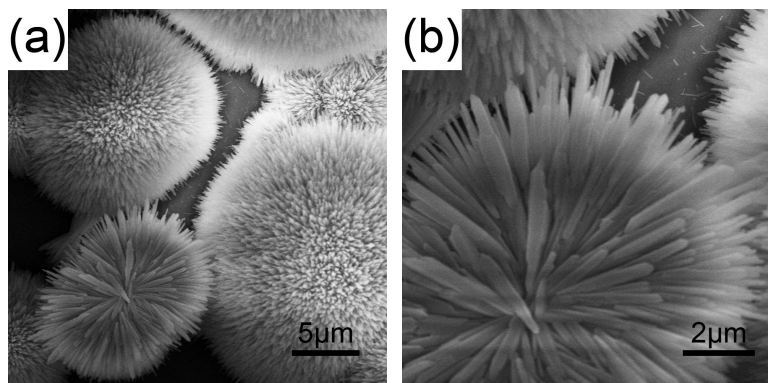
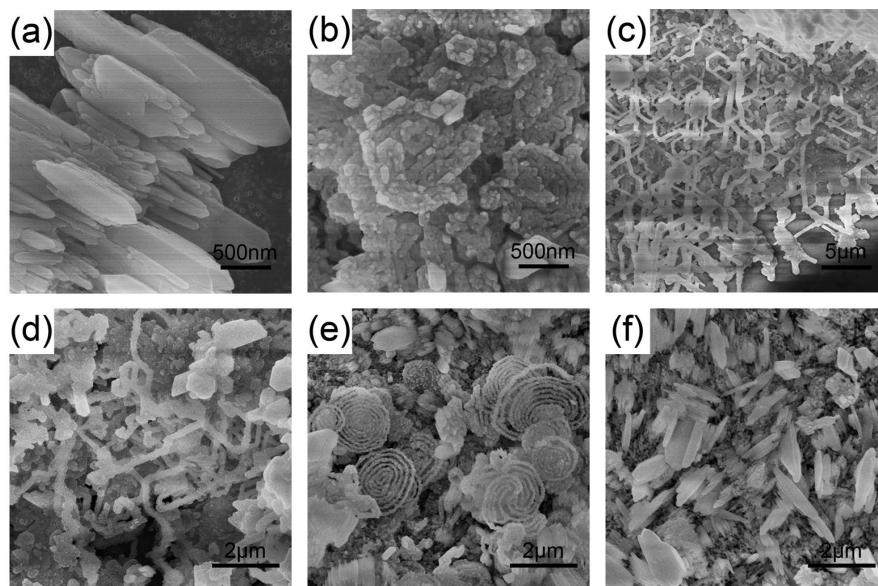**Figure S4.** SEM images of $BaCO_3$ crystals formed in 1.0 g/L polymer solution at 25 ^{o}C.

Electronic Supplementary Material (ESI) for Chemical Communications
This journal of (c) The Royal Society of Chemistry 2012

2.5 The influence of the Ba^{2+} and micelle concentrations on the morphology of $BaCO_3$ crystals

When the Ba^{2+} concentration varies, significant changes in the morphology as well as the crystal structure are observed as shown in Figure S5a-c. When the Ba^{2+} concentration is 20 mM, rods with lengths of several hundred nanometers were obtained (Figure S5a). As shown in Figure S5b, the rods are compact arranged at a lower Ba^{2+} concentration of 10 mM. With further decreasing the Ba^{2+} concentration to 2 mM, the morphology changes to fibers with tens micrometers lengths (Figure S5c).

Figure S5d-f show the morphologies of crystals prepared at various micelle concentrations. The structures transform from fibers to spirals, and then to rods with decreasing of micelle concentration from 2.0 g/L to 0.1 g/L.

Figure S5. SEM images of $BaCO_3$ crystals formed in polymer micelle solution with various micelle and barium ion concentration at 50 °C. (a) [polymer] = 1.0 g/L, [Ba^{2+}] = 20 mM; (b) [polymer] = 1.0

g/L, $[Ba^{2+}]$ = 10 mM; (c) [polymer] = 1.0 g/L, $[Ba^{2+}]$ = 2 mM; (d) [polymer] = 2.0 g/L, $[Ba^{2+}]$ = 5 mM;

(e) [polymer] = 0.3 g/L, $[Ba^{2+}]$ = 5 mM; (f) [polymer] = 0.1 g/L, $[Ba^{2+}]$ = 5 mM.

Electronic Supplementary Material (ESI) for Chemical Communications
This journal of (c) The Royal Society of Chemistry 2012

2.6 Mixture systems of alkaline earth carbonate in the presence of polymer micelles

As can be seen in Figure S5b, nanorods are formed at a Ba^{2+} concentration of 10 mM. While the introduction of Mg^{2+} (Figure S6a) or Sr^{2+} (Figure S6b) to the $BaCO_3$ mineralization system leads to the formation of spirals with fine appearances.

The Sr^{2+} can inhibit the solution nucleation. Thus the PILP phase can be stabilized long enough for the SPS process, benefiting for the one-dimensional growth. Because Ba^{2+} and Sr^{2+} have similar chemical properties and dimensions, the product is an isomorphism of $SrCO_3$ and $BaCO_3$, which are both in the orthorhombic system. So the curling behavior of the belts is similar to the $BaCO_3$ as described in the Scheme 1. Taken together, the adding of the Sr^{2+} in the $BaCO_3$ mineralization is helpful for the growth of spiral structure.
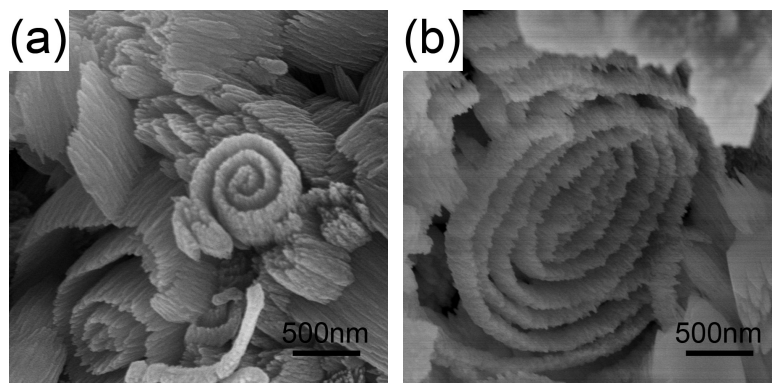

Figure S6. SEM images of alkaline earth carbonates formed in the micelle solution at 50 °C, (a) Ba-MgCO$_3$, $[Mg^{2+}] = 1$ mM, $[Ba^{2+}] = 10$ mM; (b) Ba-SrCO$_3$, $[Sr^{2+}] = 1$ mM, $[Ba^{2+}] = 10$ mM. The polymer micelle concentration is 1.0 g/L.

Electronic Supplementary Material (ESI) for Chemical Communications
This journal of (c) The Royal Society of Chemistry 2012

2.7 Ba-Sr carbonate formed in the micelle solution

Figure S7a shows a spiral wound around an irregular crystal, duplicating the overall shape. The formed belt also acts as a template and can lead to the formation a group of parallel belts (Figure S7b). As shown in Figure S7c, the spirals can occasionally alter their directions (indicated with white arrows). The belts in the sloping spirals always reverse their direction when they touch the surface of the glass slide (Figure S7d). It seems that a belt tends to change its growth direction when it hits an obstacle.
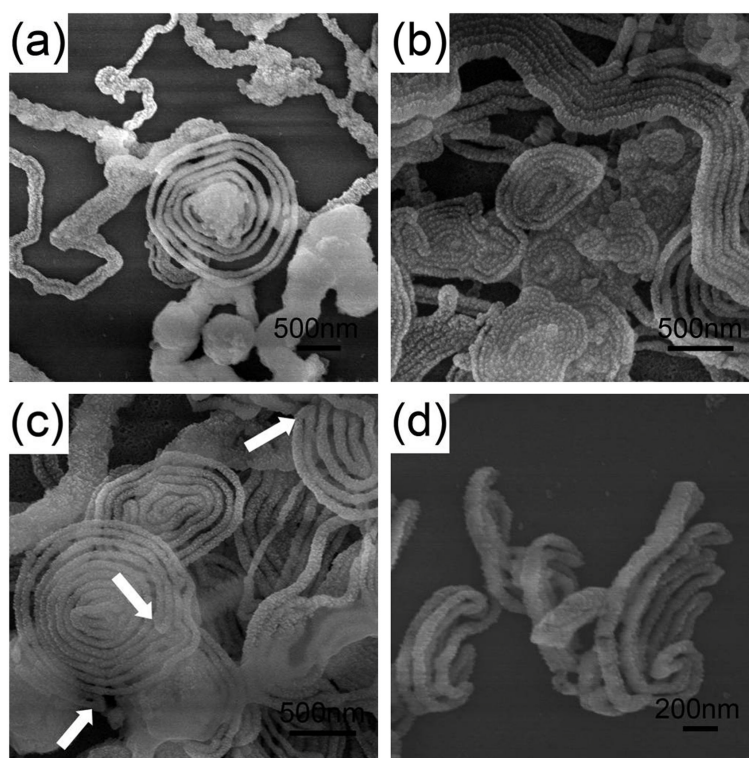
Figure S7. SEM images of the Ba-Sr system formed in the micelle solution at 50 ^{o}C. The initial concentration of Ba^{2+} and Sr^{2+} are 5 mM in all cases.

Electronic Supplementary Material (ESI) for Chemical Communications
This journal of (c) The Royal Society of Chemistry 2012

2.8 The formation process of the fiber and rod witherite crystals

Scheme S1 shows the formation process of the fibers and rods. PILP phase of $BaCO_3$ was formed in the initial stage. With a high [Polymer]/[Ba^{2+}] ratio, the PILP phase are be stabilized long enough for the SPS process (Pathway 1). The curling of the fiber is inhibited probably due to a low concentration differential of PILP phase around the growth point. Fibers are generated in this case, corresponding to the Figure S5c and S5d. While in the condition of a low [Polymer]/[Ba^{2+}] ratio, the PILP droplets crystallize directly to form rods (Pathway 2), as can be seen in the Figure S5a and S5f.
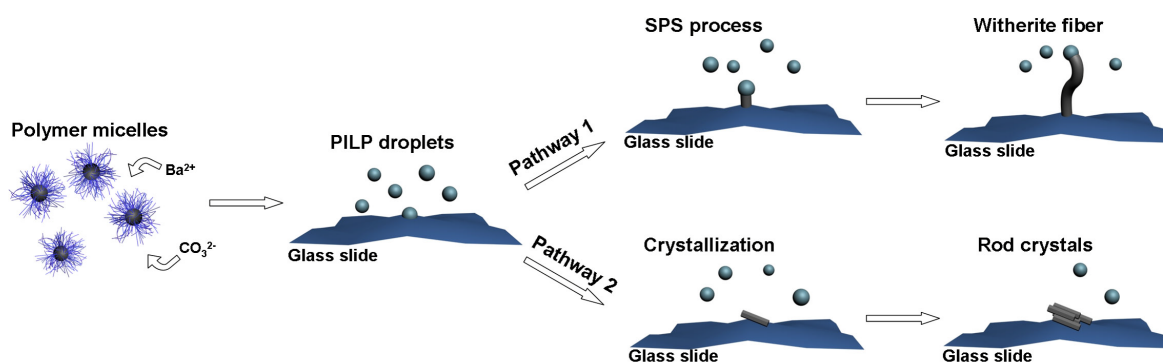
Scheme S1. Schematic image of the formation process of the fiber and rod witherite crystals.

Electronic Supplementary Material (ESI) for Chemical Communications
This journal of (c) The Royal Society of Chemistry 2012

References

(S1).   E. R. Blout, R. H. Karlson, *J. Am. Chem. Soc.*, **1956**, *78*, 941-946.

(S2).   J. Rao, Z. Luo, Z. Ge, H. Liu, S. Liu, *Biomacromolecules*, **2007**, *8*, 3871-3878.

(S3).   G. Chen, A. S. Hoffman, *Nature*, **1995**, *373*, 49-52.

(S4).   C. Cai, L. Zhang, J. Lin, L. Wang, *J. Phys. Chem. B*, **2008**, *112*, 12666-12673.

(S5).   J. Rodríguez-Hernández, S. Lecommandoux, *J. Am. Chem. Soc.*, **2005**, *127*, 2026-2027.

(S6).   S. Albeck, S. Weiner, L. Addadi, *Chem. Eur. J.*, **1996**, *2*, 278-284.